Perspective

α-Diimine Ni-Catalyzed Ethylene Polymerizations: On the Role of Nickel(I) Intermediates

Igor E. Soshnikov *[ID], **Nina V. Semikolenova, Konstantin P. Bryliakov and Evgenii P. Talsi**

Boreskov Institute of Catalysis, Pr. Lavrentieva 5, 630090 Novosibirsk, Russia; nvsemiko@catalysis.ru (N.V.S.);
bryliako@catalysis.ru (K.P.B.); talsi@catalysis.ru (E.P.T.)
* Correspondence: soshnikov@catalysis.ru

Abstract: Nickel(II) complexes with bidentate N,N-α-diimine ligands constitute a broad class of promising catalysts for the synthesis of branched polyethylenes via ethylene homopolymerization. Despite extensive studies devoted to the rational design of new Ni(II) α-diimines with desired catalytic properties, the polymerization mechanism has not been fully rationalized. In contrast to the well-characterized cationic Ni(II) active sites of ethylene polymerization and their precursors, the structure and role of Ni(I) species in the polymerization process continues to be a "black box". This perspective discusses recent advances in the understanding of the nature and role of monovalent nickel complexes formed in Ni(II) α-diimine-based ethylene polymerization catalyst systems.

Keywords: monovalent nickel; α-diimines; branched polyethylene; NMR; EPR; active species

1. Introduction

Currently, a variety of highly branched elastomeric polyethylenes (PEs) is produced by co-polymerization of ethylene with linear α-olefins such as propene, 1-butene, 1-hexene, and 1-octene [1]. The synthesis of branched PE via ethylene homopolymerization is more attractive both from economic and technological perspectives, since such approaches do not require the use of expensive pure α-olefins. Brookhart and co-workers introduced Ni(II) complexes with N,N-bidentate α-diimine ligands [2], capable of producing branched PE from ethylene as the only feedstock. Since this pioneering discovery, the area has advanced greatly, with the modifications of α-diimine ligands (by tuning both the backbone and substituents) and adjusting proper polymerization conditions providing access to polymers with desired molecular (molecular weight and molecular weight distribution, degree of branching) and mechanical characteristics [3–20].

For the rational design of Ni(II) α-diimine catalysts with the desired properties (activity, thermal stability, molecular weight characteristics and microstructure of the produced PEs), detailed understanding of the reaction mechanism and of the structure–properties relationships is a prerequisite. The key role of Ni(II)-alkyl complexes as active sites of ethylene polymerization was disclosed by Brookhart and co-workers almost 20 years ago [21], and has been extensively corroborated in further studies [22–24]. However, although Ni(I) species have been found to be ubiquitous in such systems, their nature and role have remained unclear until recently [25–32]. In the present perspective, we survey the existing experimental data, related to the structure of the monovalent nickel species formed in Ni(II) α-diimine-based catalyst systems, and discuss their possible roles in the ethylene polymerization process.

2. Cationic Ni(II) α-Diimine Complexes in Ethylene Polymerization

In 1999, Brookhart and co-workers introduced the first family of cationic Ni(II) complexes of the type $[\mathbf{L}Ni^{II}Me(X)]^+[BAr'_4]^-$ (where $\mathbf{L} = \mathbf{L^1}$ or $\mathbf{L^5}$, X = H$_2$O or Et$_2$O, and Ar' = 3,5-C$_6$H$_3$(CF$_3$)$_2$) (Figure 1, Scheme 1) [21]. According to the results of in situ ^{1}H NMR experiments, ethylene addition to the samples containing $[\mathbf{L}Ni^{II}Me(X)]^+[BAr'_4]^-$

led to ligand X displacement by C_2H_4 molecule, followed by monomer insertion into the Ni^{II}-CH_3 bond and further enchainment of the Ni^{II}-alkyl moiety. The reaction between $[L^1Ni^{II}Me(Et_2O)]^+[BAr'_4]^-$ and C_2H_4 is shown in Scheme 1.
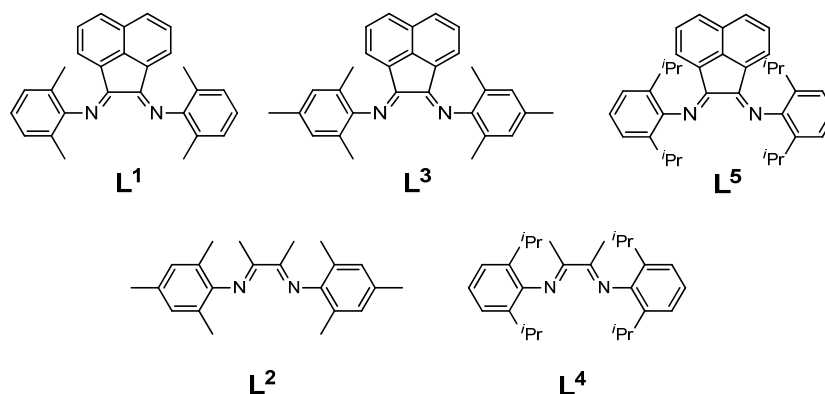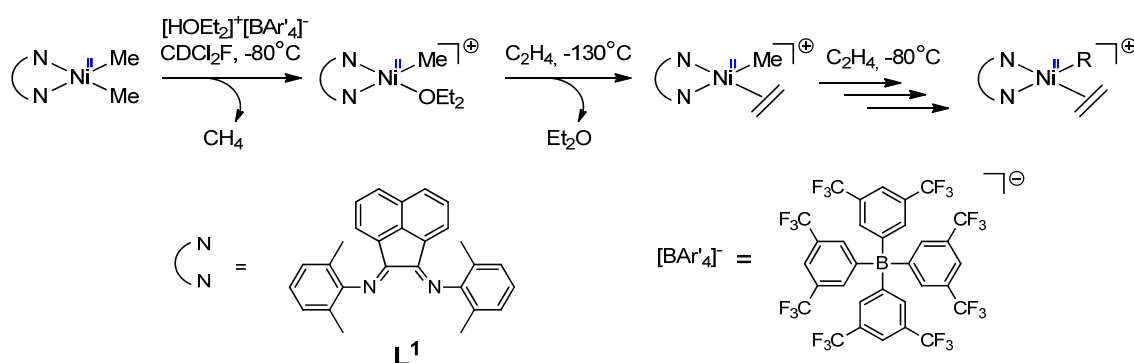

Figure 1. Structures of α-diimine ligands considered in the present work.

Scheme 1. Ethylene coordination, insertion, and polymer chain growing in the model catalyst system $[L^1Ni^{II}Me(Et_2O)]^+[BAr'_4]^-/C_2H_4$ (Ar' = 3,5-$C_6H_3(CF_3)_2$) [21].

These findings clearly demonstrate the key role of cationic Ni(II)-alkyl complexes as the active species of ethylene polymerization. Further studies of agostic interactions between the Ni(II) center and the β-H proton of the Ni^{II}-alkyl moiety in the cationic parts of the ion pairs $[L^1Ni^{II}R]^+[BAr'_4]^-$ (R = Et, Pr, ^iPr) corroborated the "chain-walking" mechanism leading to formation of branched PE [33,34] (Scheme 2), previously proposed by Fink and Mohring for Ni(II) aminobis(imino)phosphorane catalysts [35].
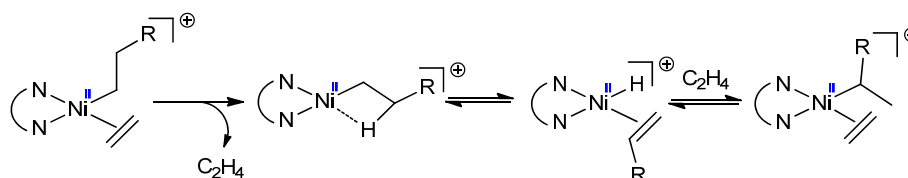
Scheme 2. Chain-walking mechanism of Me-branch formation in the course of Ni(II) α-diimine catalyzed ethylene polymerization [33].

More recently, structurally related cationic Ni(II) complexes of "real" catalyst systems such as $L^2Ni^{II}Br_2/MAO$, $L^2Ni^{II}Br_2/MMAO$ (Schemes 1 and 3; MAO—methylalumoxane, MMAO—methylalumoxane, modified by Al^iBu_3), and $L^3Ni^{II}Br_2/Al_2R_3Cl_3$ (R = Me or Et) were identified by NMR spectroscopy [24,36]. Complex $[L^2Ni^{II}-^tBu]^+[MeMMAO]^-$ was observed in the $L^2Ni^{II}Br_2/MMAO$ catalyst system at $-20\,°C$, whereas in the $L^2Ni^{II}Br_2/MAO$ one, heterobinuclear dimethyl-bridged congener $[L^2Ni^{II}(\mu\text{-}Me)_2AlMe_2]^+[MeMAO]^-$ was

detected under the same conditions (Scheme 3). Both these species could play the role of direct precursors of the active sites of ethylene polymerization. However, in the absence of ethylene, $[\mathbf{L^2}Ni^{II}\text{-}^tBu]^+[MeMMAO]^-$ and $[\mathbf{L^2}Ni^{II}(\mu\text{-}Me)_2AlMe_2]^+[MeMAO]^-$ reduce to the monovalent nickel compounds at temperatures higher than $-20\,^\circ C$ [24], which suggests that complexes of nickel(I) can also exist at higher temperatures, i.e., under practical polymerization conditions. Therefore, it is important to monitor the formation (and subsequent transformations) of nickel(I) species in "real" catalyst systems and reveal their possible role(s) in the catalytic cycle.
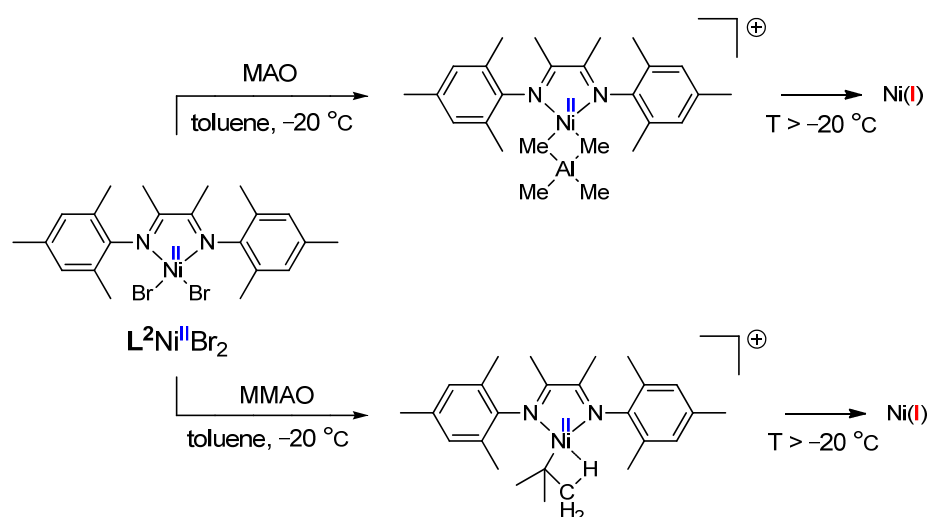
Scheme 3. Cationic Ni(II)-alkyl complexes formation in "real" catalyst systems $\mathbf{L^2}Ni^{II}Br_2$/MAO and $\mathbf{L^2}Ni^{II}Br_2$/MMAO.

3. Ni(I) α-Diimine Complexes in Ethylene Polymerization

Despite the generally recognized role of Ni(II)-alkyl complexes as the active sites of ethylene polymerization, the nature and role of Ni(I) complexes in polymerization continues to be a subject of extensive studies [25–32,37,38]. Because of the lower tolerance (compared with Ni(II) counterparts) of Ni(I) α-diimine complexes to trace amounts of moisture and oxygen, the number of examples of their successful isolation and characterization has been limited [31,32,39–43].

In 2007, Reiger and co-workers synthesized two dinuclear monovalent nickel complexes $[(\mathbf{L^4}Ni^IBr)_2MgBr_2(THF)_2]$ and $[(\mathbf{L^4}Ni^IBr)_2]$ (Figure 2) and tested them in ethylene homopolymerization [32]. According to the results of catalytic studies, $[(\mathbf{L^4}Ni^IBr)_2MgBr_2(THF)_2]$ and $[(\mathbf{L^4}Ni^IBr)_2]$ did not display any detectable polymerization activity, but adding an excess of $AlMe_3$ converted them into "polymerization-active species". The mechanism of formation of the active Ni(II) species was not established; however, the authors hypothesized that the latter could be accounted for by disproportionation of the type $Ni^I = 1/2Ni^{II} + 1/2Ni^0$.
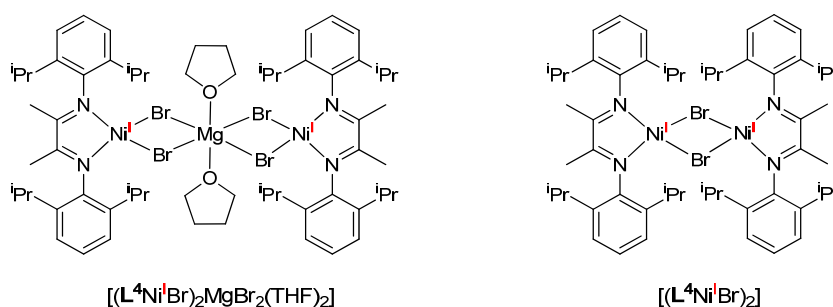

Figure 2. Structures of $[(\mathbf{L^4}Ni^IBr)_2MgBr_2(THF)_2]$ and $[(\mathbf{L^4}Ni^IBr)_2]$.

In 2015, Gao and Mu and co-workers isolated a neutral heterobinuclear nickel(I) complex [$\mathbf{L^5}$Ni^I(μ-Br)$_2$AlMe$_2$] from the $\mathbf{L^5}$Ni^{II}Br$_2$/AlMe$_3$ reaction mixture (Scheme 4, Al/Ni = 4/1) [31]. When activated with excess AlMe$_3$ or MAO, [$\mathbf{L^5}$Ni^I(μ-Br)$_2$AlMe$_2$] displayed high ethylene polymerization activity, comparable with those of $\mathbf{L^5}$Ni^{II}Br$_2$/AlMe$_3$ and $\mathbf{L^5}$Ni^{II}Br$_2$/MAO systems. It was proposed that the active Ni(II) center was formed by the intramolecular electron transfer from Ni(I) to the redox non-innocent α-diimine ligand to form the [$\mathbf{L^{5(•-)}}$Ni^{II}(μ-Me)$_2$AlMe$_2$] species (Scheme 4).
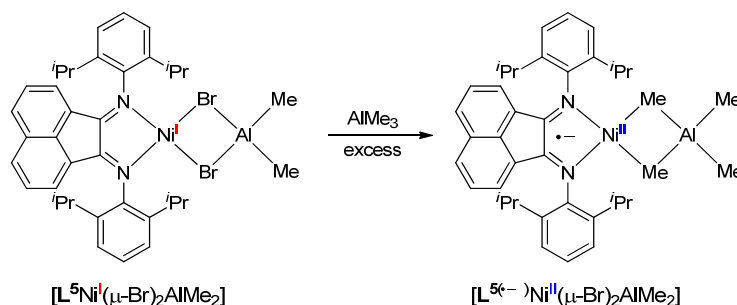
Scheme 4. Structures of [$\mathbf{L^5}$Ni^I(μ-Br)$_2$AlMe$_2$] and [$\mathbf{L^{5(•-)}}$Ni^{II}(μ-Me)$_2$AlMe$_2$].

Chirik and co-workers prepared mixed-valence Ni(I)−Ni(II) ion pairs [$\mathbf{L^1}$Ni(μ-H)]$_2$[BAr′$_4$] and [$\mathbf{L^4}$Ni(μ-H)]$_2$[BAr′$_4$] (Ar′ = 3,5-C$_6$H$_3$(CF$_3$)$_2$) that demonstrated catalytic activity in the polymerization of hexene regioisomers (1-hexene, *trans*-2-hexene, *trans*-3-hexene) when activated with MAO or Et$_2$AlOEt (Figure 3) [42].
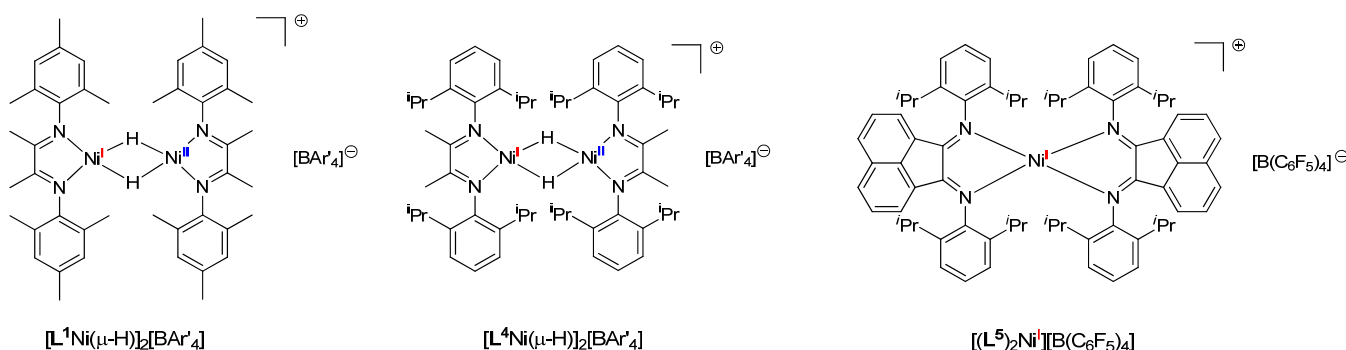

Figure 3. Structures of [$\mathbf{L^1}$Ni(μ-H)]$_2$[BAr′$_4$], [$\mathbf{L^4}$Ni(μ-H)]$_2$[BAr′$_4$], and [($\mathbf{L^5}$)$_2$Ni^I][B(C$_6$F$_5$)$_4$] (Ar′ = 3,5-C$_6$H$_3$(CF$_3$)$_2$).

Gao and co-workers prepared and characterized cationic bis-ligated complex [($\mathbf{L^5}$)$_2$Ni^I][B(C$_6$F$_5$)$_4$], which displayed moderate ethylene polymerization activity when activated with AlMe$_3$ (Figure 3) [37].

Generation of monovalent nickel complexes in the catalyst systems in situ via one-electron reduction of Ni(II) precursors seems to be an easier approach to the investigation of the role of Ni(I) species in the ethylene polymerization process, provided that side products of reduction or (and) traces of the starting material do not significantly affect the catalytic behavior. Various one-electron reducing agents can be successfully used for the quantitative conversion of Ni(II) complexes to the corresponding Ni(I) counterparts [43].

Long and co-workers investigated the effect of addition of cobaltocene Cp$_2$Co (a widely used one-electron reducing agent) on the catalytic properties of $\mathbf{L^5}$Ni^{II}Br$_2$/MAO system [44]. It was found that gradual increase of the Co/Ni ratio from 0 to 1 was accompanied by a 30% decrease of the degree of branching (from 114 to 88 branches/1000 C), while the catalytic activity did not significantly change. To establish the change of nickel spin state in the course of the reaction of $\mathbf{L^5}$Ni^{II}Br$_2$ with cobaltocene, an EPR spectrum of the sample $\mathbf{L^5}$Ni^{II}Br$_2$/Cp$_2$Co (Co/Ni = 1, toluene) was recorded. Single resonance at *g* = 2.342,

characteristic of Ni(I) (*S* = 1/2) species, with uncoupled spin localized at the metal center, was detected at −196 °C. The structure of this complex was not disclosed.

Another original approach to one-electron reduction of Ni(II) center in the $L^5Ni^{II}Br_2$/MAO system is based on using photoreductants as stoichiometric one-electron donors, followed by exposing to visible light [45]. Adding the photoreductant (*fac*-Ir(ppy)$_3$ = tris[2-phenylpyridinato-C^2,N] iridium(III)) to the system $L^5Ni^{II}Br_2$/MAO allowed achieving partial reduction, with the degree of reduction depending of the exposure time. Like in the case of $L^5Ni^{II}Br_2$/Cp$_2$Co/MAO system, the reduction of the Ni(II) center to the monovalent state leads to a drop of the degree of branching (from 111 to 93 branches/1000 C) of the resulting PE.

The explanation for the observed PE branching variation was suggested in 2020 by Roy with coworkers [38]. Computational studies have shown that Ni(II) species of the type $L^{5(\bullet-)}Ni^{II}(\mu$-Me)$_2$AlMe$_2$ rather than $L^5Ni^I(\mu$-Me)$_2$AlMe$_2$ congeners operate in the catalyst system $L^5Ni^{II}Br_2$/Cp$_2$Co/MAO. By analogy with $[L^1Ni^{II}R]^+$ species, observed by Brookhart and co-workers, it is assumed that complexes with the proposed structure $L^{5(\bullet-)}Ni^{II}R$ act as the active sites of ethylene polymerization in these systems. Although the uncoupled electron was preferentially localized at the *α*-diimine ligand, small fraction of electron density at the metal center weakened the agostic interaction between Ni and *β*-H proton of the growing polymeryl chain, thus suppressing the *β*-hydride abstraction and hence restricting the degree of chain-walking, responsible for the formation of branches (Scheme 2).

Using EPR spectroscopy in situ, Petrovskii and co-workers documented rapid and quantitative reduction of the Ni(II) center to Ni(I) state upon activation with 20 equiv. of MAO in toluene at room temperature [29]. The resulting catalyst system was active in ethylene polymerization, with the ethylene consumption rate profile typical for the majority of homogeneous polymerization catalysts, with high initial polymerization rate (90 kg·mol$_{Ni}^{-1}$·bar^{-1}·h^{-1}) followed by gradual rate decay. The EPR spectra witnessed resonances of two types of paramagnetic species. The nearly axial frozen-solution signal (g_1 = 2.22, $g_2 \approx g_3$ = 2.08) was tentatively assigned to a heterobinuclear $L^5Ni^I(\mu$-X)$_2$AlX$_2$ complex (the nature of X group was not specified), whereas a multiplet at *g* = 2.0 with partially resolved hyperfine structure (hfs) from one aluminum and two nitrogen nuclei was ascribed to aluminum species $L^{5(\bullet-)}AlX_2$, the product of irreversible *α*-diimine ligand transfer to the co-catalyst.

The nature of monovalent nickel species formed upon Ni(II) *α*-diimines activation with MMAO and AlMe$_3$ were extensively studied using ^{1}H, ^{2}H NMR and EPR spectroscopy in situ by Soshnikov and Talsi and co-workers [25–27]. When $L^4Ni^{II}Br_2$ complex, containing bulky *o*-^{i}Pr-substituents, was activated with AlMe$_3$, two types of paramagnetic heterobinuclear Ni(I) complexes, $L^4Ni^I(\mu$-Br)(μ-Me)AlMe$_2$ and $L^4Ni^I(\mu$-Me)$_2$AlMe$_2$, were detected and characterized by NMR and EPR (Scheme 5, top). Using ^{2}H-enriched AlMe$_3$ made it possible to assign the key ^{1}H and ^{2}H NMR resonances of the AlMe$_2$ moiety of $L^4Ni^I(\mu$-Br)(μ-Me)AlMe$_2$, which confirmed its heterobinuclear nature. In the case of $L^2Ni^{II}Br_2$ with *α*-diimine ligand L^2 containing less bulky Me-substituents (Figure 1), only dimethyl-bridged heterobinuclear complex $L^2Ni^I(\mu$-Me)$_2$AlMe$_2$ was detected in the $L^2Ni^{II}Br_2$/AlMe$_3$ reaction solution (Scheme 5, bottom).

Using MMAO as activator for $L^4Ni^{II}Br_2$ led to a mixture of heterobinuclear complexes $L^4Ni^I(\mu$-Br)(μ-Me)AlR$_2$ and $L^4Ni^I(\mu$-Me)$_2$AlR$_2$ at Al/Ni = 25 (R = Me or ^{i}Bu), with only the latter species existing in the reaction solution at high Al/Ni ratios (Al/Ni > 100). In the case of the $L^2Ni^{II}Br_2$/MMAO sample, only $L^2Ni^I(\mu$-Me)$_2$AlR$_2$ was present, even at Al/Ni = 25. These results are in line with the hypothesis of Petrovskii and co-workers on the nature of Ni(I) species formed in LNi^{II}Br$_2$/MAO catalyst systems.
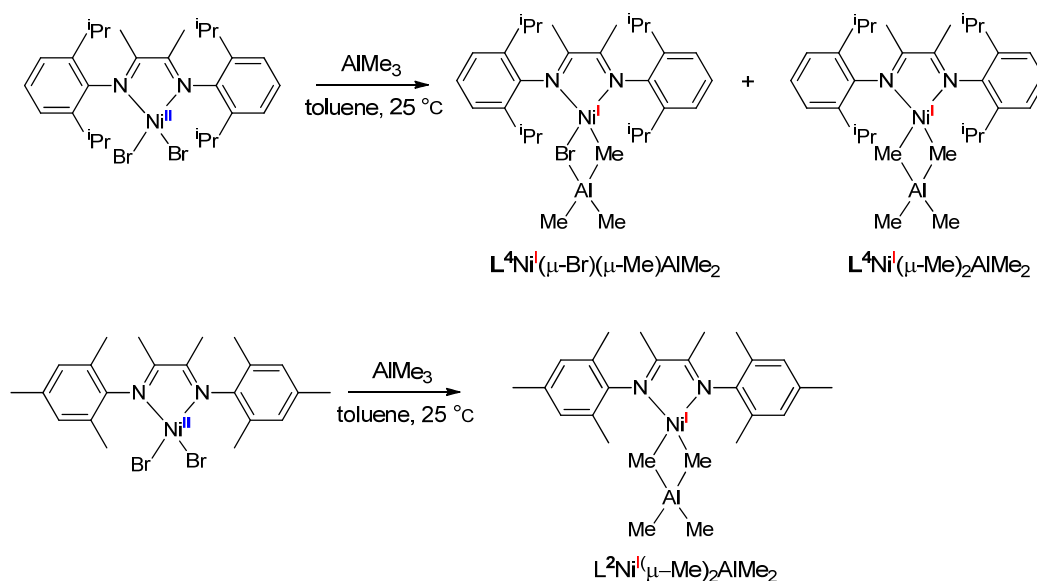
Scheme 5. Structures of complexes $L^4Ni^I(\mu\text{-Br})(\mu\text{-Me})AlMe_2$ and $L^4Ni^I(\mu\text{-Me})_2AlMe_2$ formed in the system $L^4Ni^{II}Br_2/AlMe_3$ (**top**) and of $L^2Ni^I(\mu\text{-Me})_2AlMe_2$ formed in the system $L^2Ni^{II}Br_2/AlMe_3$ (**bottom**).

Besides Ni(I) complexes, well-resolved EPR multiplets of $L^{2(\bullet-)}AlR_2$ were detected in the systems $L^2Ni^{II}Br_2/AlMe_3$ and $L^2Ni^{II}Br_2/MMAO$ (Figure 4). The propensity to the α-diimine ligand scrambling (from Ni to Al) strongly depends on the ligand structure. Indeed, the concentration of $L^{4(\bullet-)}AlR_2$ in the systems $L^4Ni^{II}Br_2/AlMe_3$ and $L^4Ni^{II}Br_2/MMAO$ was significantly higher than that of $L^{2(\bullet-)}AlR_2$ in the systems $L^2Ni^{II}Br_2/AlMe_3$ and $L^2Ni^{II}Br_2/MMAO$ at the same Ni/Al molar ratio. Combining $L^2Ni^{II}Br_2$ with Al^iBu_3 at +25 °C leads to complete ligand transfer from Ni to Al even at relatively low Ni/Al ratios (Ni/Al $\geq$ 10). The system $L^2Ni^{II}Br_2/Al^iBu_3$ showed no activity in ethylene polymerization, thus providing indirect evidence in favor of the catalyst deactivation via $L^{2(\bullet-)}AlR_2$ formation.
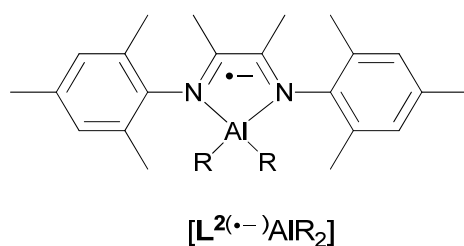
$[L^{2(\bullet-)}AlR_2]$

Figure 4. The structure of $L^{2(\bullet-)}AlR_2$, formed in the systems $L^2Ni^{II}Br_2/AlMe_3$ or $L^2Ni^{II}Br_2/MMAO$ (R = Me or ^iBu).

Dimethyl-bridged nickel(I) complexes $L^2Ni^I(\mu\text{-Me})_2AlR_2$ (R = Me or ^iBu) ultimately formed both in the $L^2Ni^{II}Br_2/MMAO$ and $L^2Ni^{II}Br_2/AlMe_3$ catalyst systems at high Al/Ni ratios (Al/Ni $\geq$ 500). To elucidate the role of these species in the ethylene polymerization process, a series of catalytic experiments was performed. Both $L^2Ni^{II}Br_2/MMAO$ and $L^2Ni^{II}Br_2/AlMe_3$ displayed high ethylene polymerization activity, yielding branched PE (Table 1).

Table 1. Ethylene polymerization data for the catalyst systems $\mathbf{L^2Ni^{II}Br_2}$/MMAO and $\mathbf{L^2Ni^{II}Br_2}$/AlMe$_3$ [a].

Entry	Activator	Activity [b]	M_n [c]	M_w/M_n	Branches/1000 C [d]
1	MMAO	3.7	39	1.9	40 ± 2
2	AlMe$_3$	2.7	39	2.0	36 ± 2
3 [e]	MMAO	1.5	38	2.3	39 ± 2
4 [f]	AlMe$_3$	1.3	46	2.2	36 ± 2

[a] Polymerization conditions: heptanes (200 mL) for entries 1, 3 and toluene (100 mL) for entries 2, 4; time 60 min; T = 50 °C; P(C$_2$H$_4$) = 5 bar; 2.0 μmol of pre-catalyst $\mathbf{L^2Ni^{II}Br_2}$; Al/Ni = 500. [b] In 10^6 g PE/(mol$_{Ni}$·h). [c] In 10^3 g/mol; measured by GPC. [d] Measured by ^{1}H NMR. [e] Complex $\mathbf{L^2Ni^{II}Br_2}$ was mixed with 20 eq. of MMAO in heptanes, stored during 1 h at 25 °C, and then introduced in the reactor. [f] Complex $\mathbf{L^2Ni^{II}Br_2}$ was mixed with 10 eq. of AlMe$_3$ in toluene, stored during 1 h at 25 °C, and then introduced in the reactor.

The time profiles of the rates of ethylene consumption by the systems $\mathbf{L^2Ni^{II}Br_2}$/MMAO and $\mathbf{L^2Ni^{II}Br_2}$/AlMe$_3$ were typical for the majority of homogeneous polymerization catalysts, with high initial polymerization rate followed by gradual activity decay (Figure 5a). The systems containing $\mathbf{L^2Ni^{I}(\mu\text{-}Me)_2AlR_2}$ (R = Me or ^{i}Bu), generated in situ by preliminary quantitative reduction of $\mathbf{L^2Ni^{II}Br_2}$ with 10 equiv. of AlMe$_3$ or 20 equiv. of MMAO, demonstrated a dramatically different catalytic behavior.
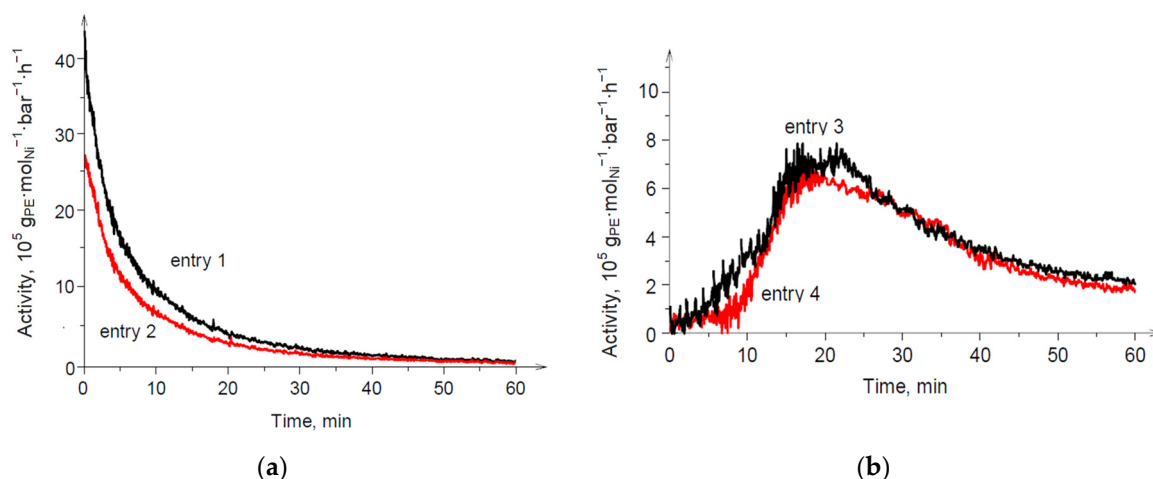
Figure 5. Ethylene consumption rate time profiles for the catalyst systems $\mathbf{L^2Ni^{II}Br_2}$/MMAO (entry 1), $\mathbf{L^2Ni^{II}Br_2}$/AlMe$_3$ (entry 2) (**a**), and $\mathbf{L^2Ni^{II}Br_2}$+MMAO (20 equiv)/MMAO (entry 3), $\mathbf{L^2Ni^{II}Br_2}$+AlMe$_3$ (10 equiv)/AlMe$_3$ (entry 4) (**b**).

Indeed, one can distinguish three regions in ethylene consumption time profiles of the $\mathbf{L^2Ni^{I}(\mu\text{-}Me)_2AlR_2}$/MMAO and $\mathbf{L^2Ni^{I}(\mu\text{-}Me)_2AlMe_2}$/AlMe$_3$ systems: the initial activity increase from zero to maximum values within 10–15 min, followed by stationary ethylene consumption during the next 10 min, which eventually turns into gradual decline (Figure 5b). The measured (average) catalytic activities of the systems $\mathbf{L^2Ni^{I}(\mu\text{-}Me)_2AlR_2}$/MMAO and $\mathbf{L^2Ni^{I}(\mu\text{-}Me)_2AlMe_2}$/AlMe$_3$ were twice as low as those of the systems $\mathbf{L^2Ni^{II}Br_2}$/MMAO and $\mathbf{L^2Ni^{II}Br_2}$/AlMe$_3$. Crucially, the molecular characteristics of the polymers obtained were virtually the same (Table 1), thus witnessing the same, single-site, catalytically active species in both cases. In contrast to the results of Long and co-workers [44], complete reduction of Ni(II) to Ni(I) had no effect on the degree of PE branching. We believe that the observed kinetic peculiarities (namely, the initial induction period, Figure 5b) and polymer properties (Table 1) could be accounted for by the disproportionation pathway Ni^I = 1/2Ni^{II} + 1/2Ni^0, previously proposed by Reiger and co-workers [32], rather than by intramolecular electron transfer $\mathbf{L^2Ni^{I}(\mu\text{-}Me)_2AlR_2} \rightarrow \mathbf{L^{2(\bullet-)}Ni^{II}(\mu\text{-}Me)_2AlR_2}$.

Therefore, the $\mathbf{L^2Ni^{I}(\mu\text{-}Me)_2AlR_2}$ species observed in $\mathbf{L^2Ni^{II}Br_2}$/MMAO and $\mathbf{L^2Ni^{II}Br_2}$/AlMe$_3$ should be considered as catalyst resting state rather than deactivation products. To rationalize the mechanism of transformation of $\mathbf{L^2Ni^{I}(\mu\text{-}Me)_2AlR_2}$ resting states into the Ni(II) active sites in the presence of ethylene, the system $\mathbf{L^2Ni^{II}Br_2}$/MMAO/C$_2$H$_4$ was stud-

ied by EPR spectroscopy [27]. Before ethylene addition to the sample $\mathbf{L^2Ni^{II}Br_2}$/MMAO (Al/Ni = 25), the resonances of $\mathbf{L^2Ni^I}$(μ-Me)$_2$AlR$_2$ with nearly axial *g*-factor anisotropy (g_1 = 2.208, g_2 = 2.060, g_3 = 2.050) were detected in the frozen solution (−196 °C) EPR spectrum (Figure 6a). Noticeably, the perpendicular component ($g^\perp = g_2 \approx g_3$) displayed a partially resolved hfs from two nitrogen atoms of the α-diimine ligand ($a(^{14}N)$ = 1.06 mT). Upon the addition of ca. 600 equiv. of C$_2$H$_4$ at −70 °C, partial conversion of $\mathbf{L^2Ni^I}$(μ-Me)$_2$AlR$_2$ to a new Ni(I) complex **A** with dramatically different frozen-solution EPR-parameters ($g_1 \approx g_2$ = 2.34, $g_3 \approx 1.99$) was observed (Figure 6b). At temperatures higher than −70 °C, ethylene was rapidly consumed (with PE formation), accompanied by disappearance of **A** and restoration of the initial concentration of $\mathbf{L^2Ni^I}$(μ-Me)$_2$AlR$_2$.
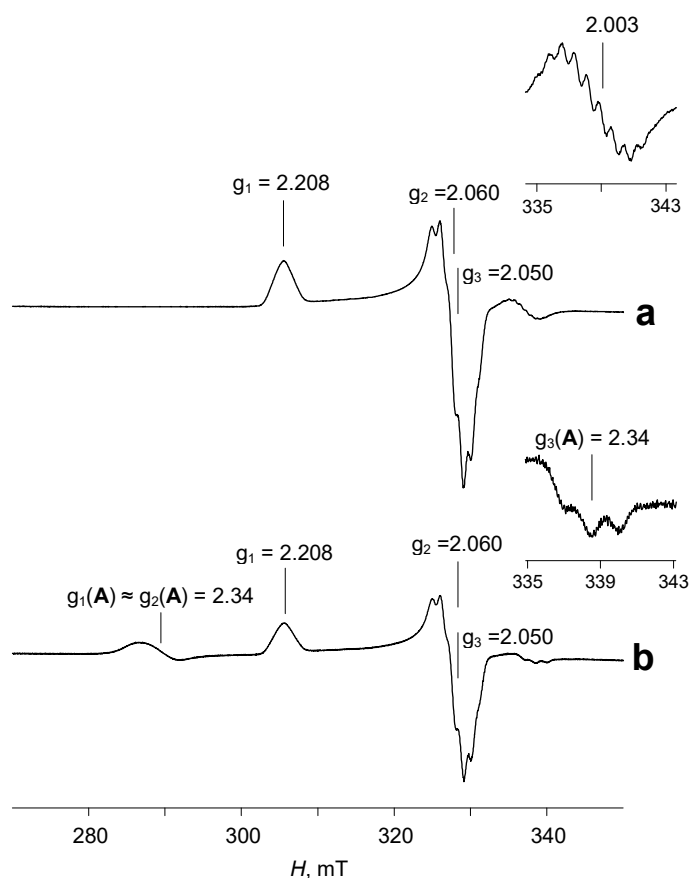
Figure 6. Frozen solution EPR spectra (−196 °C) of the samples: (**a**) $\mathbf{L^2Ni^{II}Br_2}$/MMAO (Al/Ni = 25, toluene, [Ni] = 10 mM), mixed and stored for 1 h at 25 °C; (**b**) sample in (**a**) after adding 600 equiv. of ethylene at −70 °C.

Remarkably, the parallel component ($g_\parallel = g_3 \approx 1.99$) of the frozen solution EPR spectrum of **A** displayed hfs from only one nitrogen atom ($a(^{14}N)$ = 1.51 mT). This is evidence of dramatic reorganization of the first coordination sphere of the paramagnetic center in the course of $\mathbf{L^2Ni^I}$(μ-Me)$_2$AlR$_2$ conversion into **A**. Quantitative return of **A** into $\mathbf{L^2Ni^I}$(μ-Me)$_2$AlR$_2$ after ethylene consumption, apparently, reflects reversible ethylene coordination to Ni, with the α-diimine ligand remaining coordinated to Ni in both complexes. Based on the above data, **A** was tentatively assigned to an ethylene adduct of the type $\mathbf{L^2Ni^I}$(C$_2$H$_4$)R (R = Me or ^{i}Bu). Further studies are planned to reliably establish the structure of this adduct and evaluate its chemical reactivity.

4. Conclusions

Complexes of nickel(II) with bidentate *N,N*-donor α-diimine ligands, introduced by Brookhart and co-workers [2], have established themselves as promising catalysts for the

preparation of valuable polymeric products, such as branched elastomeric polyethylene and copolymers of ethylene with polar monomers. Meanwhile, despite considerable efforts, detailed understanding of the catalytic mechanism has not been achieved as yet.

In their pioneering studies, Brookhart and co-workers disclosed the key role of cationic nickel(II)-alkyl complexes of the type $[\mathbf{L}\mathrm{Ni}^{II}\mathrm{R}]^+[\mathrm{A}]^-$ ($\mathbf{L}$ = α-diimine ligand, R = polymeryl, $[\mathrm{A}]^-$ = counter-ion) in the polymer chain growth. However, in-depth investigations witness that monovalent nickel species may prevail in the catalyst systems under "real" polymerization conditions. For example, in situ NMR and EPR studies of the Ni(I) species formed in "real" catalytic systems ($\mathbf{L}\mathrm{Ni}^{II}\mathrm{Br}_2$/MMAO and $\mathbf{L}\mathrm{Ni}^{II}\mathrm{Br}_2$/AlMe$_3$; $\mathbf{L}$ = α-diimine ligand) have demonstrated the prevalence of neutral heterobinuclear complexes of the type $\mathbf{L}\mathrm{Ni}^{I}(\mu\text{-Me})_2\mathrm{AlR}_2$ (where R = Me or ^{i}Bu) in the reaction solution. However, until recently, their role in the catalytic process has remained unexplored.

The observations of the reactivity of α-diimine Ni(I) complexes (either isolated or generated in the reaction mixture in situ) toward ethylene (affording branched PEs) indicated that monovalent nickel species should not be discounted as potential active species or, more plausibly, their direct precursors.

The mechanism of Ni(I) conversion to the active divalent state in the course of ethylene polymerization continues to be debated controversially. On the one hand, intramolecular one-electron transfer from the Ni(I) to the redox non-innocent α-diimine ligand ($\mathbf{L}\mathrm{Ni}^{I}(\mu\text{-Me})_2\mathrm{AlR}_2 \rightarrow \mathbf{L}^{(\bullet-)}\mathrm{Ni}^{II}(\mu\text{-Me})_2\mathrm{AlR}_2$) can yield the catalytically active, formally "Ni(II)" sites. On the other hand, the occurrence of disproportionation of the type $\mathrm{Ni}^{I} = 1/2\mathrm{Ni}^{II} + 1/2\mathrm{Ni}^{0}$ in the course of polymerization cannot be excluded, either. Further studies are needed to distinguish between these possibilities. In either case, however, these complexes of monovalent nickel can play important roles as precursors of active species and/or catalyst resting state rather than the products of the catalyst deactivation. We foresee further progress in understanding the mechanistic landscape of α-diimine nickel(II)-based catalysts of ethylene polymerization, and try to contribute to it in the near future.

Author Contributions: All authors have read and agreed to the published version of the manuscript.

Conflicts of Interest: The authors declare no conflict of interest.

References

1. McKnight, A.L.; Waymouth, R.M. Group 4 ansa-Cyclopentadienyl-Amido Catalysts for Olefin Polymerization. *Chem. Rev.* **1998**, *98*, 2587–2598. [CrossRef] [PubMed]
2. Johnson, L.K.; Killian, C.M.; Brookhart, M. New Pd(II)- and Ni(II)-Based Catalysts for Polymerization of Ethylene and α-Olefins. *J. Am. Chem. Soc.* **1995**, *117*, 6414–6415. [CrossRef]
3. Zhong, L.; Li, G.L.; Liang, G.D.; Gao, H.Y.; Wu, Q. Enhancing thermal stability and living fashion in α-diimine-nickel catalyzed (co)polymerization of ethylene and polar monomers by increasing the steric bulk of ligand backbone. *Macromolecules* **2017**, *50*, 2675–2682. [CrossRef]
4. Wang, Z.; Liu, Q.B.; Solan, G.A.; Sun, W.-H. Recent advances in Ni$_{\mathrm{imine}}$-donor ligand effects on catalytic activity, thermal stability and oligo-/polymer structure. *Coord. Chem. Rev.* **2017**, *350*, 68–83. [CrossRef]
5. Chen, Z.; Brookhart, M. Exploring ethylene/polar vinyl monomer copolymerizations using Ni and Pd α-diimine catalysts. *Acc. Chem. Res.* **2018**, *51*, 1831–1839. [CrossRef] [PubMed]
6. Guo, L.H.; Lian, K.B.; Kong, W.Y.; Xu, S.; Jiang, G.R.; Dai, S.Y. Synthesis of various branched ultra-high-molecular-weight polyethylenes using sterically hindered acenaphthene-based α-diimine Ni(II) catalysts. *Organometallics* **2018**, *37*, 2442–2449. [CrossRef]
7. Fang, J.; Sui, X.L.; Li, Y.G.; Chen, C.L. Synthesis of polyolefin elastomers from unsymmetrical α-diimine nickel catalyzed olefin polymerization. *Polym. Chem.* **2018**, *30*, 4143–4149. [CrossRef]

8. Tan, C.; Chen, C.L. Emerging palladium and nickel catalysts for copolymerization of olefins with polar monomers. *Angew. Chem. Int. Ed.* **2019**, *58*, 7192–7200. [CrossRef] [PubMed]

9. Liao, Y.D.; Zhang, Y.X.; Cui, L.; Mu, H.L.; Jian, Z.B. Pentiptycenyl substituents in insertion polymerization with α-diimine nickel and palladium species. *Organometallics* **2019**, *38*, 2075–2083. [CrossRef]

10. Gong, Y.F.; Li, S.K.; Gong, Q.; Zhang, S.J.; Liu, B.Y.; Dai, S.Y. Systematic investigations of ligand steric effects on α-diimine nickel catalyzed olefin polymerization and copolymerization. *Organometallics* **2019**, *38*, 2919–2926. [CrossRef]

11. Soshnikov, I.E.; Bryliakov, K.P.; Antonov, A.A.; Talsi, E.P. Ethylene polymerization of nickel catalysts with α-diimine ligands: Factors controlling the structure of active species and polymer properties. *Dalton Trans.* **2019**, *48*, 7974–7984. [CrossRef]

12. Liang, T.; Goundari, S.B.; Chen, C. A simple and versatile nickel platform for the generation of branched high molecular weight polyolefins. *Nat. Commun.* **2020**, *11*, 372. [CrossRef] [PubMed]

13. Xia, J.; Zhang, Y.X.; Kou, S.Q.; Jian, Z.B. A concerted double-layer steric strategy enables an ultra-highly active nickel catalysts to access ultrahigh molecular weight polythylens. *J. Catal.* **2020**, *90*, 30–36. [CrossRef]

14. Tran, Q.H.; Brookhart, M.; Daugulis, O. New neutral nickel and palladium sandwich catalysts: Synthesis of ultrahigh molecular weight polyethylene (UHMWPE) via highly controlled polymerization and mechanistic studies of chain propagation. *J. Am. Chem. Soc.* **2020**, *142*, 7198–7206. [CrossRef] [PubMed]

15. Hu, X.Q.; Wang, C.Q.; Jian, Z.B. Comprehensive studies of ligand electronic effect on unsymmetrical α-diimine nickel(II) promoted ethylene (co)polymerizations. *Polym. Chem.* **2020**, *11*, 4005–4012. [CrossRef]

16. Li, S.K.; Xu, S.Y.; Dai, S.Y. A remote nonconjugated electron effect in insertion polymerization with α-diimine nickel and palladium species. *Polym. Chem.* **2020**, *11*, 2692–2699. [CrossRef]

17. Muhammad, Q.; Tan, C.; Chen, C.L. Concerted steric and electronic effects on α-diimine nickel- and palladium-catalyzed ethylene polymerization and copolymerization. *Sci. Bull.* **2020**, *65*, 300–307. [CrossRef]

18. Hu, X.Q.; Zhang, Y.X.; Jian, Z.B. Unsymmetrical strategy makes significant differences in α-diimine nickel and palladium catalyzed ethylene copolymerizations. *ChemCatChem* **2020**, *12*, 2497–2505. [CrossRef]

19. Dai, S.Y.; Li, S.K.; Xu, G.Y.; Wu, C.; Liao, Y.D.; Guo, L.H. Flexible cycloalkyl substituents in insertion polymerization with α-diimine nickel and palladium species. *Polym. Chem.* **2020**, *11*, 1393–1400. [CrossRef]

20. Antonov, A.A.; Bryliakov, K.P. Post-metallocene catalysts for the synthesis of ultrahigh molecular weight polyethylene: Recent advances. *Eur. Polymer J.* **2021**, *142*, 110162. [CrossRef]

21. Svejda, S.A.; Johnson, L.K.; Brookhart, M. Low-Temperature Spectroscopic Observation of Chain Growth and Migratory Insertion Barriers in (α-Diimine)Ni(II) Olefin Polymerization Catalysts. *J. Am. Chem. Soc.* **1999**, *121*, 10634–10635. [CrossRef]

22. Antonov, A.A.; Samsonenko, D.G.; Talsi, E.P.; Bryliakov, K.P. Formation of Cationic Intermediates upon the Activation of Bis(imino)pyridine Nickel Catalysts. *Organometallics* **2013**, *32*, 2187–2191. [CrossRef]

23. Soshnikov, I.E.; Semikolenova, N.V.; Zakharov, V.A.; Moller, H.M.; Olscher, F.; Osichow, A.; Gottker-Schnettmann, I.; Mecking, S.; Talsi, E.P.; Bryliakov, K.P. Formation and Evolution of Chain-Propagating Species Upon Ethylene Polymerization with Neutral Salicylaldiminato Nickel(II) Catalysts. *Chem. Eur. J.* **2013**, *19*, 11409–11417. [CrossRef] [PubMed]

24. Soshnikov, I.E.; Semikolenova, N.V.; Bryliakov, K.P.; Antonov, A.A.; Zakharov, V.A.; Talsi, E.P. NMR spectroscopic identification of Ni(II) species formed upon activation of (α-diimine)NiBr₂ polymerization catalysts with MAO and MMAO. *Dalton Trans.* **2018**, *47*, 4968–4974. [CrossRef] [PubMed]

25. Soshnikov, I.E.; Semikolenova, N.V.; Bryliakov, K.P.; Antonov, A.A.; Sun, W.H.; Talsi, E.P. Nature of Heterobinuclear Ni(I) Complexes Formed upon the Activation of the α-Diimine Complex LNi^{II}Br₂ with AlMe₃ and MMAO. *Organometallics* **2021**, *40*, 907–914. [CrossRef]

26. Soshnikov, I.E.; Semikolenova, N.V.; Bryliakov, K.P.; Antonov, A.A.; Sun, W.H.; Talsi, E.P. Activation of an α-diimine Ni(II) precatalysts with AlMe₃ and Al(iBu)₃: Catalytic and NMR and EPR spectroscopic studies. *Organometallics* **2020**, *39*, 3034–3040. [CrossRef]

27. Soshnikov, I.E.; Semikolenova, N.V.; Bryliakov, K.P.; Antonov, A.A.; Sun, W.H.; Talsi, E.P. EPR spectroscopic study of Ni(I) species in the catalyst system for ethylene polymerization based on α-diimine Ni(II) complex activated by MMAO. *J. Organomet. Chem.* **2019**, *880*, 267–271. [CrossRef]

28. Gurinovich, N.S.; Petrovsky, S.K.; Saliy, I.V.; Saraev, V.V. Influence of a diimine ligand and an activator on the processes taking place in Brookhart-type nickel catalytic systems. *Res. Chem. Intermed.* **2018**, *44*, 1935–1944. [CrossRef]

29. Gurinovich, N.S.; Petrovskii, S.K.; Saraev, V.V.; Salii, I.V. Study of the Nature and Mechanism of the Formation of Paramagnetic Species in Nickel-Based Brookhart-Type Catalytic Systems. *Kinet. Catal.* **2016**, *57*, 523–527. [CrossRef]

30. Titova, Y.Y.; Belykh, L.B.; Schmidt, F.K. EPR Spectroscopy of catalytic systems based on nickel complexes of 1,4-diaza-1,3-butadiene (alpha-diimine) ligands in hydrogenation and polymerization reactions. *Low Temp. Phys.* **2015**, *41*, 25–28. [CrossRef]

31. Gao, W.; Xin, L.; Hao, Z.; Li, G.; Su, J.H.; Zhou, L.; Mu, Y. The ligand redox behavior and role in 1,2-bis[(2,6-diisopropylphenyl)imino]-acenaphthene nickel-TMA(MAO) systems for ethylene polymerization. *Chem. Commun.* **2015**, *51*, 7004–7007. [CrossRef]

32. Meinhard, D.; Reuter, P.; Rieger, B. Activation of Polymerization Catalysts: Synthesis and Characterization of Novel Dinuclear Nickel(I) Diimine Complexes. *Organometallics* **2007**, *26*, 751–754. [CrossRef]

33. Leatherman, M.D.; Svejda, S.A.; Johnson, L.K.; Brookhart, M. Mechanistic studies of nickel(II) alkyl agostic cations and alkyl ethylene complexes: Investigations of chain propagation and isomerization in (α-diimine)Ni(II)-catalyzed ethylene polymerization. *J. Am. Chem. Soc.* **2003**, *125*, 3068–3081. [CrossRef] [PubMed]

34. Xu, H.; White, P.B.; Hu, C.; Diao, T. Structure and Isotope Effects of the β-H Agostic (α-Diimine)Nickel Cation as a Polymerization Intermediate. *Angew. Chem. Int. Ed.* **2017**, *56*, 1535–1538. [CrossRef]

35. Mohring, V.M.; Fink, G. Novel Polymerization of α-Olefins with the Catalyst System Nickel/Aminobis(imino)phosphorane. *Angew. Chem. Int. Ed.* **1985**, *24*, 1001–1003. [CrossRef]

36. Soshnikov, I.E.; Semikolenova, N.V.; Bryliakov, K.P.; Antonov, A.A.; Sun, W.H.; Talsi, E.P. The nature of nickel species formed upon the activation of α-diimine nickel(II) pre-catalyst with alkylaluminum sesquichlorides. *J. Organomet. Chem.* **2020**, *907*, 121063. [CrossRef]

37. Xu, S.; Chen, X.; Luo, G.; Gao, W. Nickel complexes based on BIAN ligands: Transformation and catalysis on ethylene polymerization. *Dalton Trans.* **2021**, *50*, 7356–7363. [CrossRef] [PubMed]

38. Chapleski, R.C., Jr.; Kern, L.; Anderson, W.C., Jr.; Long, B.K.; Roy, S. A Mechanistic Study of Microstructure Modulation in Olefin Polymerizations using a Redox-Active Ni(II) α-Diimine Catalyst. *Catal. Sci. Technol.* **2020**, *10*, 2029–2039. [CrossRef]

39. Zarate, C.; Yang, H.; Bezdek, J.M.; Hesk, D.; Chirik, P.J. Ni(I)-X Complexes Bearing a Bulky α-Diimine Ligand: Synthesis, Structure, and Superior Catalytic Performance in the Hydrogen Isotope Exchange in Pharmaceuticals. *J. Am. Chem. Soc.* **2019**, *141*, 5034–5044. [CrossRef] [PubMed]

40. Joannou, M.V.; Bezdek, M.J.; Albahily, K.; Korobkov, I.; Chirik, P.J. Synthesis and Reactivity of Reduced α-Diimine Nickel Complexes Relevant to Acrylic Acid Synthesis. *Organometallics* **2018**, *37*, 3389–3393. [CrossRef]

41. Kuang, Y.; Anthony, D.; Katigbak, J.; Marrucci, F.; Humagain, S.; Diao, T. Ni(I)-Catalyzed Reductive Cyclization of 1,6-Dienes: Mechanism-Controlled trans Selectivity. *Chem* **2017**, *3*, 268–280. [CrossRef]

42. Leonard, N.G.; Yruegas, S.; Ho, S.C.; Sattler, A.; Bezdek, M.J.; Chirik, P.J. Synthesis of cationic, dimeric α-diimine nickel hydride complexes and relevance to the polymerization of olefins. *Organometallics* **2020**, *39*, 2630–2635. [CrossRef]

43. Lin, C.Y.; Power, P.P. Complexes of Ni(I): A "rare" oxidation state of growing importance. *Chem. Soc. Rev.* **2017**, *46*, 5347–5399. [CrossRef] [PubMed]

44. Anderson, W.C., Jr.; Rhinehart, J.L.; Tennyson, A.G.; Long, B.K. Redox-Active Ligands: An Advanced Tool To Modulate Polyethylene Microstructure. *J. Am. Chem. Soc.* **2016**, *138*, 774–777. [CrossRef]

45. Kaiser, J.M.; Anderson, W.C., Jr.; Long, B.K. Photochemical regulation of a redox-active olefin polymerization catalyst: Controlling polyethylene microstructure with visible light. *Polym. Chem.* **2018**, *9*, 1567–1570. [CrossRef]